Research on optimal operation model of multi-energy complementary energy system considering multi-type peak shaving costs

Jinhong Chen[1], Chongle Chen [1], Kai Lin [1], Hua Li [2], Chuansheng Xie [2]

[1] Fujian Shuikou Power Generation Group Co., Ltd, Fuzhou 305004, China
[2] North China Electric Power University, School of Economics and Management, Beijing 102206, China

Abstract. The vigorous development of clean energy is an important way to achieve "Carbon peak, Carbon neutral", but the inherent intermittent and uncontrollable power generation characteristics of clean energy such as scenery and other comprehensive factors make the energy consumption problem more prominent, and the multi-energy complementary can solve the energy consumption problem more effectively. However, the current study of multi-energy complementary operation only considers the fuel cost, load shedding and wind and solar abandonment cost, and does not consider enough the peaking cost of thermal power units and the life loss of batteries. To address these problems, a multi-energy complementary energy system operation optimization model considering multiple types of peaking costs is established, and the peaking costs of regulating units are modeled more finely and solved by a dynamic inertia weighted particle swarm algorithm. The results demonstrate that the addition of energy storage system can effectively reduce the total operating cost of the system under the condition of large-scale clean energy grid connection, and the addition of creeping cost and low load operating cost can reflect the cost of conventional units more realistically, which can better provide the dispatching strategy for the decision of multi-energy complementary operation of power system.

Keywords: Multi-energy complementary; Integrated energy system; Peaking cost; Optimal operation; Particle swarm algorithm.

1. Introduction

In 2021, the Development and Reform Commission and the Energy Bureau issued the "Guidance on Promoting the Integration of Electricity Source, Network, Load, Storage and Multi-energy Complementary Development", proposing that in order to achieve the goal of "striving to reach the peak of carbon dioxide emissions by 2030 and striving to achieve carbon neutrality by 2060", it is necessary to improve the level of clean energy utilization and Power system operational efficiency, and promote "wind, water, fire and storage" to achieve multi-energy complementarity[1] . Making full use of and vigorously developing wind, solar, water and other renewable energy resources is an important way to achieve the "Carbon peak, Carbon neutral" goal in China[2] . With the increasing proportion of clean energy represented by wind power and photovoltaic power generation in the future power system, it is important to study the optimal scheduling of multi-energy complementary energy system for clean energy.

Multi-energy complementation is an effective way to achieve optimal integration and efficient utilization of resources by using the complementary characteristics of various energy sources[3-4] . At present, scholars at home and abroad have done a lot of exploratory work on the architecture, configuration and optimal operation of multi-energy complementary systems. The literature [5] constructs a multi-energy flow system model that mixes distributed energy conversion and storage devices and various types of loads to form a mixture of cooling, heat, electricity and gas, and then analyzes the key technologies and challenges of multi-energy complementary and integrated and optimized energy systems. In the literature [6], an electric-thermal-hydrogen multi-energy complementary system was constructed to explore the optimal operation of the multi-energy complementary system from three aspects: hydrogen production from renewable energy electrolytic water, hydrogen storage technology, and hydrogen-fired gas turbine technology. In the literature [7], an operationally integrated optimization model of a terminal-type multi-energy complementary system integrating solar, wind, and natural gas was established, and the effects of optimization objectives and energy prices on the optimal configuration and performance of the system were investigated. With the development of energy storage technology, the role of energy storage in multi-energy complementary energy systems has received the attention of many scholars[8] . In

the literature [9], a full-life cycle two-layer optimization model for cooling, heating and power storage scheduling planning was developed to study the profitable strategies of cooling, heating, power and hybrid energy storage in the case of multi-energy complementary operation of combined cooling, heating and power supply (CCHP) units and electric refrigeration and other equipment, and the economics and feasibility of system configuration with different energy storage were discussed. In the literature [10], a multi-objective optimal operation model of a multi-energy complementary system coupled with wind power, photovoltaic, hydroelectric, thermal power and energy storage devices is constructed to study the complementary characteristics of different power sources in the coupled system and the role of the operation mode of the energy storage system. In the literature [11], a mixed integer linear programming model considering system constraints such as renewable energy abandonment rate and operational constraints for each power plant is developed to analyze the optimal battery and thermal energy storage capacity of a multi-energy complementary system integrating wind power, photovoltaic, concentrated solar power and batteries. In the literature [12], a hybrid wind-photovoltaic-thermal-storage multi-energy complementary system was developed to analyze the optimal scheduling strategy of the system with the objectives of optimizing economic efficiency, maximizing reliability, minimizing renewable energy power fluctuations, and best conforming to the renewable energy generation schedule. In the literature [13], an economic dispatch model of microgrid containing wind, solar, storage, micro gas turbine, diesel generator and fuel cell considering the battery life was developed and solved by applying a mixed integer linear programming algorithm. In the literature [14], based on the analysis of peak compensation and peak sharing, a complementary coordinated optimal scheduling strategy of wind-water-fire-storage multi-energy system is proposed considering the peak regulation initiative constraint of thermal power units.

Existing studies on the optimal operation of multi-energy complementary energy systems only consider the fuel cost, load shedding and wind and solar abandonment costs, but not enough consideration is given to the peaking cost of thermal units and the life loss of batteries. Therefore, in this paper, we establish an optimization model for the operation of clean energy multi-energy complementary energy systems, and model the peaking cost of the regulating units in a more refined way, in which the thermal units are considered for low load conditions, ramp-up, start-stop, and the battery life loss, and use the dynamic inertia weighted particle swarm algorithm to solve. Finally, the cost of optimal operation of the multi-energy complementary system under different scenarios is studied in a region of Fujian, and the role of energy storage system in a high percentage of renewable energy grid-connected power system and the actual cost of conventional units are analyzed.

2. Energy system operation optimization model for clean energy multi-energy complementary

2.1 Objective function

In order to cope with the power system scenario of grid-connected renewable energy with high percentage of random variation, this paper establishes a mathematical model of the total operating cost of the multi-energy complementary optimal dispatch system containing five types of energy sources: wind, solar, fire, storage and storage, with the objective of minimizing the system operating cost. The objective function is as follows.

$$f(x)=\min\sum_{i=1}^{N}\left(C_i^T+C_i^B+C_i^{PC}+C_i^{LS}\right) \quad (1)$$

In the formula: i is the operation time period, $i=1,2,\cdots,N$; N is the total operation time period; C_i^T , C_i^B , C_i^{PC} , C_i^{LS} are the thermal unit operation cost, battery loss cost, wind/solar abandonment penalty cost and system load shedding penalty cost in the i time period, respectively.

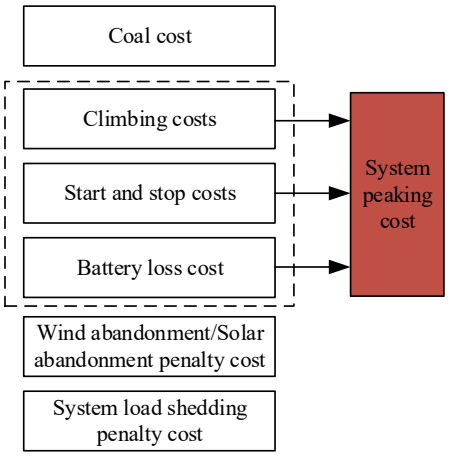

Figure 1 System operating costs

2.1.1 Thermal power unit costing function

Faced with a high proportion of wind and solar with random volatility to the grid, in order to smooth out the volatility of wind and solar and meet the national energy strategy demand of limiting wind and solar abandonment, thermal power units are bound to face frequent climbing, frequent start and stop or often run under the new operating conditions of deep peaking. The traditional quadratic formula does not consider the impact of new operating conditions of thermal power units on operating costs. Therefore, this paper proposes a cost calculation method that takes into account the new operating conditions of thermal units for the grid-connected scenario with a high proportion of renewable energy.

(1) Cost of coal combustion

The coal combustion cost calculation function is as follows.

$$C_i^{T1}=\begin{cases}\sum_{l=1}^{N}\left|a\left(P_i^T\right)^2+b\left(P_i^T\right)+c\right| & \alpha\times P_{\max}^T\le P_i^T\le P_{\max}^T\\ \sum_{T=1}^{N}\left|p\left(P_i^T\right)^3+(a+q)\left(P_i^T\right)^2+(b+m)P_i^T+(c+n)\right| & P_{\min}^T\le P_i^T\le\alpha\times P_{\max}^T\end{cases} \tag{2}$$

In the formula: P_i^T is the thermal unit output at i; a, b, c are the conventional coal cost factors; p, q, m, n are the low-load operating cost factors; α are the low-load operating boundary limits.

(2) Climbing cost

The cost function of thermal power units is not only related to the output of the units, but also directly related to the climbing rate of the units at the adjacent time. The cost function of thermal power unit is not only related to the output of the unit, but also directly related to the climbing rate of the unit in the adjacent time. The climbing cost calculation function is as follows.

$$C_i^{T2}=\sum_{i=1}^{N}\gamma\left|\frac{\mathrm{d}P_i^T}{\mathrm{d}t}\right| \tag{3}$$

In the formula: γ is the creep cost factor for thermal power units.

(3) Start/stop cost

The start-up and shutdown cost functions for thermal power units are shown below.

$$C_i^{T3}=\sum_{i=1}^{N}n_iS_i^T \tag{4}$$

In the formula: n_i is the cost of starting and stopping thermal units in the i time period; S_i^T is the number of starting and stopping thermal units in the i time period.

2.1.2 Battery wear and tear costing function

The cycle life of the battery is short, generally use 1~3a will have to be replaced, so in the actual operation must consider the battery life loss, calculate its loss cost. The loss of the battery is mainly affected by the depth of discharge and the amount of fatigue cycle. The battery loss cost calculation function is shown below.

$$C_i^B=\frac{W}{Q^{life}\sqrt{\eta_{rt}}} \tag{5}$$

$$Q_i^{life}=DOD_i\frac{u_iq_{\max}V}{1000} \tag{6}$$

In the formula: Q_i^{life} is the full life output of the battery; η_{rt} is the round trip efficiency of the battery; DOD_i is the depth of discharge of the battery; u_i is the fatigue cycle of the battery; $q_{\max}$ is the maximum capacity of the battery; V is the normal operating voltage of the battery.

2.1.3 Costing function for wind/solar abandonment penalty

In order to improve the grid penetration of wind and solar energy and meet the requirements of national energy strategy, a wind/solar abandonment penalty cost calculation model is introduced to ensure the required penetration ratio of wind and solar, and the penalty cost is calculated according to formula (8).

$$C_i^{PC}=\sum_{i=1}^{N}\lambda P_i^{PC} \tag{7}$$

In the formula: λ is the wind/solar cost penalty factor; P_i^{PC} is the wind/solar power abandoned in the i time period.

2.1.4 Cut load penalty costing function

To ensure grid stability and power quality, when the actual system output deviates from the load demand, a load shedding penalty cost calculation function shall be introduced, as shown in formula (8), to accept the penalty according to the magnitude of the deviation.

$$C_i^{LS}=\sum_{i=1}^{N}\beta P_i^{LS} \tag{8}$$

In the formula: β is the load shedding cost penalty factor; P_i^{LS} is the load shedding power in the i time period.

2.2 Binding Conditions

2.2.1 Thermal Power Unit Constraints

The output constraint of thermal power unit is shown in formula (9), and formula (10) represents the upward and downward climbing rate limits of thermal power unit.

$$P_{\min}^T\le P_i^T\le P_{\max}^T \tag{9}$$

$$-\Delta P_T^{down}\le\left(P_i^T-P_{i-1}^T\right)\le\Delta P_T^{up} \tag{10}$$

In the formula: $P_{\min}^T$ and $P_{\max}^T$ are the minimum and maximum output of thermal power unit respectively; ΔP_T^{down} and ΔP_T^{up} are the maximum downward and upward climbing rates of thermal power unit respectively. The minimum continuous operation/shutdown time constraint for thermal power units is shown in formula (11).

$$\begin{cases}T_{it}^{on}\ge T_{\min}^{on}\\ T_{it}^{off}\ge T_{\min}^{off}\end{cases} \tag{11}$$

In the formula: T_{it}^{on} and T_{it}^{off} are the cumulative start-up and shut-down times of thermal power units respectively; $T_{\min}^{on}$ and $T_{\min}^{off}$ are the minimum continuous start-up and shut-down times of thermal power units respectively.

2.2.2 Wind power and photovoltaic unit constraints

The output constraints of wind and PV units are shown in formulas (12) and (13), respectively.

$$0 \le P_i^W \le P_{\max}^W \tag{12}$$

$$0 \le P_i^{PV} \le P_{\max}^W \tag{13}$$

In the formula: P_i^W, P_i^{PV} are the actual output of wind and solar in the i time period respectively; $P_{\max}^W$, $P_{\max}^{PV}$ are the maximum output of wind and solar in the i time period respectively.

2.2.3 *Pumped storage plant constraints*

The pumped storage unit power generation and pumping power constraints are shown in formulas (14) and (15), and formula (16) is the water balance constraint for pumped storage power plants.

$$0 \le P_i^{PH} \le P_{\max}^{PH} \tag{14}$$

$$0 \le P_i^{PP} \le P_{\max}^{PH} \tag{15}$$

$$\sum_{i=1}^{T_G}\left(P_i^{PH} > 0\right) = -\eta \sum_{i=1}^{N-T_G}\left(P_i^{PH} < 0\right) \tag{16}$$

In the formula: P_i^{PH} and P_i^{PP} are the power generation and pumping power of the pumped storage plant in the i time period, respectively; $P_{\max}^{PH}$ and $P_{\max}^{PP}$ are the rated power generation and pumping power of the pumped storage plant, respectively; η is the pumped storage conversion efficiency; T_G is the operating time period of the pumped storage power generation.

2.2.4 Battery Constraints

The power constraint of the electrochemical energy storage plant is shown in formulas (17) and (18).

$$0 \le P_i^C \le P_{\max}^C \tag{17}$$

$$0 \le P_i^B \le P_{\max}^B \tag{18}$$

In the formula: P_i^C, P_i^B are the battery charging and discharging power in i time period respectively; $P_{\max}^C$, $P_{\max}^B$ are the maximum battery charging and discharging power respectively.

The power constraint of the battery is shown in formula (19), and formula (20) is the power balance constraint of the battery.

$$W_{\min}^B \le W_i^B \le W_{\max}^B \tag{19}$$

$$W_{i+1}^B = W_i^B + P_i^B \Delta t \tag{20}$$

In the formula: $W_{\min}^B$ and $W_{\max}^B$ are the minimum and maximum remaining battery power respectively; W_i^B is the remaining battery power in the i time period.

3. Dynamic inertia weighted particle swarm algorithm

The particle swarm algorithm is a new evolutionary algorithm developed by J Kennedy in recent years. The algorithm starts from a random solution and iteratively updates the optimal solution found by tracking the particle itself with the optimal solution currently found by the whole population to obtain the global optimal solution. The optimal scheduling problem of power grid is a high-dimensional, multi-objective, nonlinear optimization problem, and the particle swarm algorithm has the advantages of simplicity and generality, robustness, high accuracy and fast convergence, and has a strong ability of finding the optimal solution. In this paper, we introduce a linear decreasing weight strategy and use formula (21) for calculation, so that the algorithm has a higher probability of converging to the global optimal solution position.

$$\omega = \omega_{\max} - \left(\omega_{\max} - \omega_{\min}\right)\frac{t}{T_{\max}} \tag{21}$$

In the formula: $\omega_{\min}$, $\omega_{\min}$ are the minimum and maximum inertia weights respectively; t is the current iteration number of i; $T_{\max}$ is the maximum iteration number.

The basic flow of the dynamic inertia weight particle swarm algorithm is shown in Figure 2.

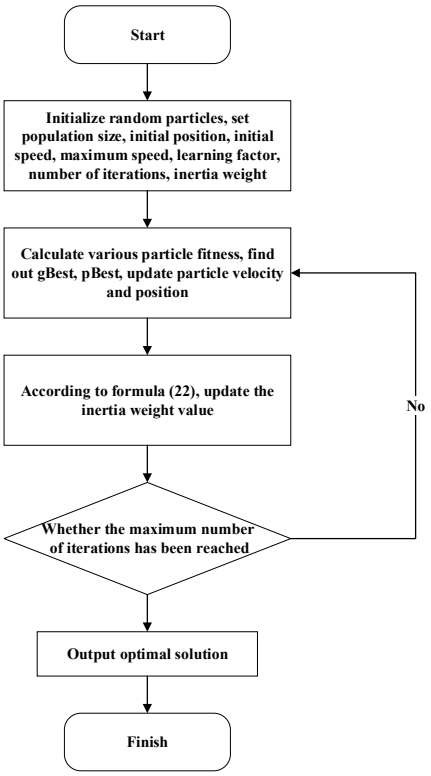

Figure 2 Flow chart of dynamic inertia weight particle swarm algorithm

4. Case study

4.1 Parameter Setting

With reference to the existing resource allocation in a region of Fujian, the installed capacity of each power source and its share in the calculation are shown in Table 1.

Table 1 Power supply types and their installed power ratio in a region of Fujian

Power supply type	Installed Capacity/MW	Power Supply %
Thermal power generation	1320	57.77
Wind Power	600	26.26
Photovoltaic power generation	250	10.94
Pumped storage	100	4.38
Electrochemical Energy Storage	15	0.72

The parameters of thermal power units of 300MW, 140MW and 100MW are used for simulation calculation. The maximum upward and downward climbing rates of thermal power units are set as ±30% of the maximum output of the units respectively; the climbing cost factor of thermal power units is set as 25; when the output of the units is lower than 70% of the rated power, it is judged as low load operation condition, i.e. α =0.7. According to the equiproportional calculation method, the coal consumption rate calculation curve applicable to the low load operation of each unit is fitted, and according to the standard coal price of RMB 500/t, the low load operation cost calculation curve is obtained as shown in Figure 2 The low load operation cost calculation curve of thermal power units is shown in Figure 3.

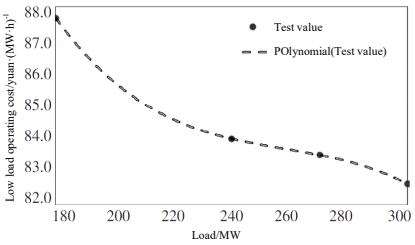

(a) 300MW thermal power unit

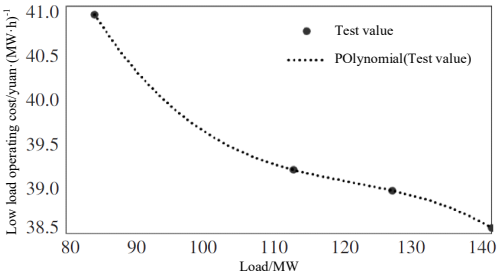

(b) 140MW thermal power unit

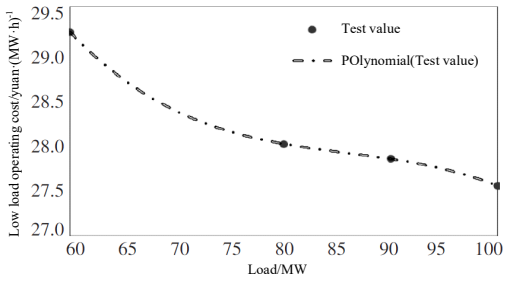

(c) 100MW thermal power unit

Figure 3 Calculation curve of low load operation cost of thermal power units

The two reversible pumped storage units have the same parameters, both with rated output of 50 MW and pumped storage conversion efficiency η = 0.75. The cost penalty factor for wind and solar abandonment is taken as λ = 200. The model is solved optimally using a dynamic inertia weight particle swarm algorithm with particle swarm size of 2000 and iteration number of 10000.

5. Example Results

In this paper, the dynamic inertia weighted particle swarm algorithm is used to solve the optimal scheduling mathematical model for the following three test scenarios: Scenario 1, wind, solar and fire multi-energy complementary optimal scheduling without energy storage in the benchmark scenario; Scenario 2, wind, solar, fire, storage and storage multi-energy complementary optimal scheduling with pumped storage and battery storage system in the benchmark scenario; Scenario 3, wind, solar, fire, storage and storage multi-energy complementary optimal scheduling with 1200MW wind and In Scenario 3, under the installed capacity of 1200MW wind power and 400MW PV, the optimal dispatching of wind, solar, fire, storage and storage with pumped storage and battery storage system is added.

In the scenario 1 condition, the day-ahead complementary optimal scheduling strategy is shown in Figure 4.

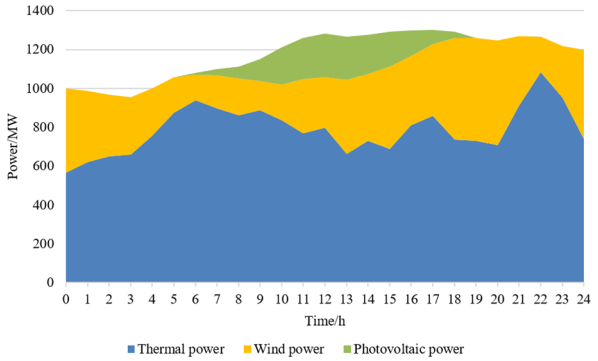

Figure 4 Optimal scheduling strategy before wind, solar and fire days under scenario 1 conditions

As can be seen from Figure 4, the scenery anti-peaking characteristics are obvious, in the 1~5 time period, the system load demand curve changes gently, but the wind power output decreases steeply; the thermal power unit is in the upward climbing operation condition, at this time,

the thermal power unit takes the main load demand. In time periods 20 and 21, PV output becomes zero, wind power output starts to show a downward trend, and thermal units are in upward climbing operation. In the 22~24 time period, the system load demand slowly decreases, but the wind power output increases significantly, and the thermal units are in downhill operation to reduce the wind and solar abandonment. In order to smooth out the scenery volatility, thermal units frequently switch between upward and downward climbing operating conditions, but the overall system peaking resources are limited. Wind and solar abandonment occurs in the time periods of 4~9 and 19~20. Two types of energy storage, pumped storage and chemical storage, are introduced for multi-energy complementary optimal dispatch. The multi-energy complementary optimal dispatching strategy under scenario 2 conditions is shown in Figure 5.

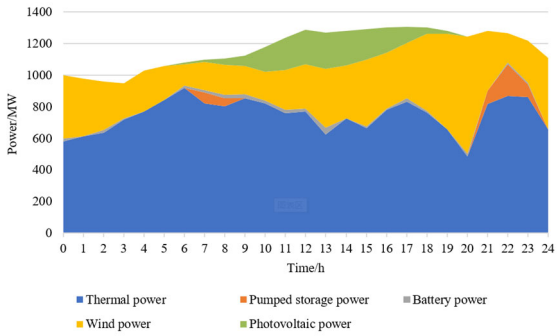

Figure 5 Optimal scheduling strategy for wind, solar, fire, storage and storage days before scenario 2 conditions

As can be seen from Figure 5, pumped storage is stored during the time periods 6~9 and 20~24, storing excess wind and solar output, and releasing energy mainly during the time periods when the scenery's anti-peaking characteristics and fluctuation characteristics are more obvious than the thermal power's insufficient peaking capacity, alleviating the system's requirement for thermal power unit peaking flexibility. The frequent dispatch of pumped storage and storage battery devices effectively smooths out the fluctuations of load and scenery, reduces the grid system's requirement for thermal unit flexibility and the impact of high proportion of renewable energy to the grid stability, and alleviates the problem of abandoned wind and solar.

In the face of the development demand of large-scale renewable energy grid-connected in China and the need of global energy strategy, multi-energy complementary optimal dispatching is required to increase the installed capacity of wind and solar. The optimal dispatching strategy of multi-energy complementary under scenario 3 is shown in Figure 6.

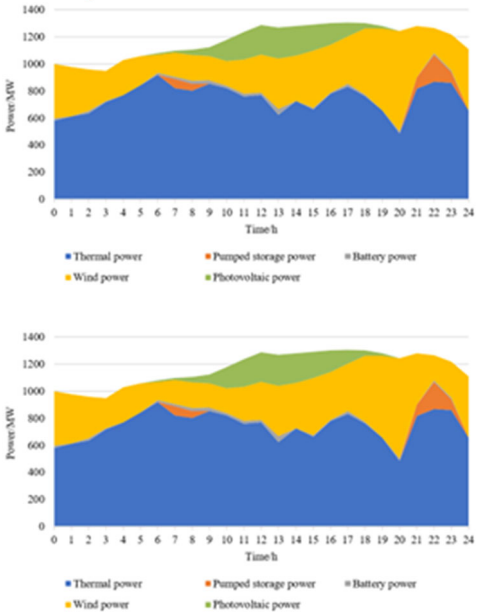

Figure 6 Optimal scheduling strategy for wind, solar, fire, storage and storage days before scenario 3 conditions

As can be seen from Figure 6, as the proportion of installed clean energy sources such as wind and solar rises, pumped storage is stored in the periods 0~1, 3-7, 9~11, 15~17, and 21~24, and is more widely involved in multi-energy optimal dispatch, and its utilization efficiency is improved. The massive use of clean energy such as wind and solar reduces the dependence of the energy system on thermal power generation, lowers the fuel cost of the system, and makes the energy system cleaner and lower carbon.

The results of the total system cost and each operating cost component of the thermal unit for the three scenarios are shown in Table 2.

Table 2 Operating costs under each scenario

Scenes	Total cost / million	Start/Stop/10,000	Conventional coal combustion / million yuan	Low-load coal combustion / million yuan	Climbing / million	Wind and solar abandonment rate/%
Scenario 1	847	109	930	1.41	1.50	6.29
Scenario 2	788	51	729	1.29	6.71	5.12
Scenario 3	663	128	531	123	1.50	15.43

Comparing scenarios 1 and 2, it can be seen that the addition of the energy storage system effectively reduces the total system operating cost and alleviates the frequent start and stop, climbing magnitude and frequent switching of climbing conditions of thermal power units due to the high scenery penetration conditions. However, due to capacity size and economic constraints, the battery peak shaving, fill the valley, smooth scenery volatility role is not as obvious as pumped storage. The increase of wind and solar installed capacity can effectively reduce the system operation cost, and scenario 3 reduces 15.81% relative to scenario 2. However, in order to smooth out the

wind and solar volatility, the number of operating condition changes of thermal power units increases, and the abandoned wind and solar rate increases due to the total capacity of system flexibility peaking resources remains unchanged, but at this time the system integrated operation cost is the lowest. In order to continue to reduce the wind and solar abandonment rate, new peaking resources need to be added.

6. Conclusion

In this paper, a more refined modeling of the peaking cost of the regulating units is carried out, in which the thermal units consider the low-load operating conditions, ramp climbing, start-stop, and the battery considers the life loss, so that the established multi-energy complementary energy system operation optimization model can reflect the system operation cost more realistically, and the dynamic inertia weight particle swarm algorithm is used. The results show that the inclusion of energy storage system effectively reduces the total system operation cost, and the inclusion of ramp climbing cost and low load operation cost can more realistically reflect the generation cost of conventional units when large-scale random volatile power sources are connected to the grid, and fully weigh the increased generation cost due to wind and solar abandonment losses and balance volatility in the dispatching process, which can better provide a better solution for the high proportion of renewable energy to the grid situation It can better provide dispatching strategies for multi-energy complementary operation of power systems with high proportion of renewable energy sources on the grid.

Acknowledgement

This study is funded by the management consulting project of Fujian Shuikou Power Generation Group Co., Ltd. (SGFJSK00DBJS2100606)

References

1. Development and Reform Commission Energy Bureau on the guidance of promoting the integration of power source, network, load and storage and the development of multi-energy complementarity [J]. Gazette of the State Council of the People's Republic of China, 2021(12):59-62.
2. Shu Yinbiao, Zhang Liying, Zhang Yunzhou, Wang Yaohua, Lu Gang, Yuan Bo, Xia Peng. Research on carbon peaking and carbon neutral pathway of China's power[J]. Strategic Study of CAE, 2021,23(06):1-14.
3. Hu Di, Ding Ming, Bi Rui, Zhang Jingjing, Pan Jing. Analysis of the impact of photovoltaic and wind power complementarity on the planning of high penetration renewable energy cluster access[J]. Proceedings of the CSEE,2020,40(03):821-836.DOI:10.13334/j.0258-8013.pcsee.182308.
4. Teng Yun,Liu Shuo,Hui Xi,Chen Zhe. A joint demand-side response model considering the synergistic optimization of regional multi-energy system clusters[J]. Proceedings of the CSEE,2020,40(22):7282-7296.DOI:10.13334/j.0258-8013.pcsee.191715.
5. Ai Qian,Hao Ran. Key technologies and challenges of multi-energy complementary and integrated optimization energy systems[J]. Automation of Electric Power Systems,2018,42(04):2-10+46.
6. Lin Li, Zheng Xin Yao, Zhou Longwen. Optimal scheduling of wind-fire-storage multi-energy complementary based on hydrogen-fired gas turbine[J/OL]. Power System Technology:1-17[2022-08-12].DOI:10.13335/j.1000-3673.pst.2022.0059.
7. CHEN Yi,XU Yingxin,XU Dongjie,GAO Xiang. Optimal configuration and performance analysis of terminal-type multi-energy complementary system[J/OL]. Power Generation Technology:1-9[2022-08-12]. https://kns-cnki-net.webvpn.ncepu.edu.cn/kcms/detail/33.1405.tk.20220314.2244.006.html
8. Li Xianfeng,Zhang Hongzhang,Zheng Qiong,Yan Jingwang,Guo Yuguo,Hu Yongsheng. Electrochemical energy storage technology in the energy revolution[J]. Bulletin of Chinese Academy of Sciences, 2019, 34(04):443-449. DOI:10.16418/j.issn.1000-3045.2019.04.009.
9. Xiong W, Liu YQ, Su Wanhuang, Hao Ran, Wang Yue, Ai Qian. Optimal configuration of multiple energy storage for regional integrated energy system considering multi-energy complementarity[J]. Electric Power Automation Equipment, 2019,39(01):118-126.DOI:10.16081/j.issn.1006-6047.2019.01.018.
10. Li P, Dond R, Wang L, et al. Multi-energy coordinated operation optimization model for wind-solar-hydro-thermal-energy storage system considering the complementary characteristics of different power resources[C] //2018 2nd IEEE Conference on Energy Internet and Energy System Integration (EI2). IEEE, 2018: 1-6.
11. Li P, Huang Y, Qi W, et al. Capacity co-optimization of thermal and battery energy storage system in multi-energy complementary system[C]//2019 IEEE Innovative Smart Grid Technologies-Asia (ISGT Asia). IEEE, 2019: 3815-3819.
12. ZHONG Yu-Feng, HUANG Min-Xiang, YE Cheng-Jin. Multi-objective operation optimization of microgrid based on dynamic scheduling of battery energy storage system[J]. Electric Power Automation Equipment,2014,34(06):114-121.
13. Liu, Chunyang, Wang, Xiuli, Liu, Shimin, Zhu, Zhenpeng, Wu, Xiong, Duan, Jie, Hou, Fei, Xie, Linhong. Economic dispatch model of microgrid accounting for battery life[J]. Electric Power

Automation Equipment,2015,35(10):29-36. DOI:10.16081/j.issn.1006-6047.2015.10.005.

14. Li Tie, Li Zhengwen, Yang Junyou, Cui Dai, Wang Zhonghui, Ma Kun, Hu Wei. Complementary coordinated optimal scheduling of wind-water-fire-storage multi-energy systems with peak regulation initiative[J]. Power System Technology, 2020, 44(10):3622-3630.DOI:10.13335/j.1000-3673.pst.2020.0626.